

# Immunotherapy for choroidal neovascularization in a laser-induced mouse model simulating exudative (wet) macular degeneration

Puran S. Bora\*, Zhiwei Hu<sup>†</sup>, Tongalp H. Tezel\*, Jeong-Hyeon Sohn\*, Shin Goo Kang\*, Jose M. C. Cruz\*, Nalini S. Bora\*, Alan Garen<sup>†‡</sup>, and Henry J. Kaplan<sup>\*‡</sup>

\*Department of Ophthalmology and Visual Sciences, University of Louisville, Louisville, KY 40202; and <sup>†</sup>Department of Molecular Biophysics and Biochemistry, Yale University, New Haven, CT 06520

Contributed by Alan Garen, December 31, 2002

Age-related macular degeneration (AMD) is the leading cause of blindness after age 55 in the industrialized world. Severe loss of central vision frequently occurs with the exudative (wet) form of AMD, as a result of the formation of a pathological choroidal neovascularization (CNV) that damages the macular region of the retina. We tested the effect of an immunotherapy procedure, which had been shown to destroy the pathological neovascularization in solid tumors, on the formation of laser-induced CNV in a mouse model simulating exudative AMD in humans. The procedure involves administering an Icon molecule that binds with high affinity and specificity to tissue factor (TF), resulting in the activation of a potent cytolytic immune response against cells expressing TF. The Icon binds selectively to TF on the vascular endothelium of a CNV in the mouse and pig models and also on the CNV of patients with exudative AMD. Here we show that the Icon dramatically reduces the frequency of CNV formation in the mouse model. After laser treatment to induce CNV formation, the mice were injected either with an adenoviral vector encoding the Icon, resulting in synthesis of the Icon by vector-infected mouse cells, or with the Icon protein. The route of injection was i.v. or intraocular. The efficacy of the Icon in preventing formation of laser-induced CNV depends on binding selectively to the CNV. Because the Icon binds selectively to the CNV in exudative AMD as well as to laser-induced CNV, the Icon might also be efficacious for treating patients with exudative AMD.

Several prevalent diseases are associated with abnormal angiogenesis and formation of a pathological neovascularization (PNV), notably cancers with solid tumors, diabetic retinopathy, and the exudative (wet) form of age-related macular degeneration (AMD). Two procedures have been described as potential treatments for PNV-associated diseases, an antiangiogenesis protocol to inhibit angiogenesis (1, 2) and an anti-PNV protocol to destroy selectively the PNV (3–6). Because a PNV usually has formed by the time the disease is diagnosed, destruction of the PNV probably will be necessary to achieve optimal therapeutic efficacy. Here we report the results of testing an anti-PNV procedure in a mouse model that simulates exudative AMD. The procedure involves administering a chimeric antibody-like molecule, called an Icon, which binds with high affinity and specificity to the receptor tissue factor (TF). TF is expressed on endothelial cells lining the luminal surface of a PNV but not of a normal vasculature (7, 8), thus providing a specific and accessible therapeutic target. The Icon is composed of factor VII (fVII), the natural ligand for TF, conjugated to the Fc domain of an IgG1 Ig. The Icon functions as an anti-TF antibody, with higher affinity and specificity than can be achieved with an anti-TF antibody. The TF–Icon complex activates a potent cytolytic immune attack mediated by natural killer cells and complement (9). Cytolysis of endothelial cells of the PNV, and possibly of other cells in the wall of a leaky PNV vessel that express TF, results in selective destruction of the PNV, as demonstrated in mouse models of solid tumors (3, 4).

Exudative AMD involves pathological angiogenesis that originates from the choroid beneath the retina to form a PNV, called a choroidal neovascularization (CNV), containing abnormal blood vessels that can leak fluid and bleed, hence the name exudative AMD. The fluid and blood released from the CNV can damage the structure and function of the overlying retina, usually in the central macular area, leading to the loss of central vision. Several procedures are currently used to treat submacular CNV, notably photodynamic therapy (10), submacular surgery (11, 12), and macular translocation (13–15). However, most treated patients do not show visual improvement, and the surgical procedures can cause serious complications. The severe visual disability caused by AMD and the lack of an adequate treatment for the disease has motivated a search for new therapeutic strategies. Here we show that formation of a laser-induced CNV can be prevented at an early stage in a mouse model, by i.v. or intraocular (i.o.) injections of either an adenoviral vector encoding the Icon or Icon protein.

## Materials and Methods

**Animals.** C57BL/6 mice 4–6 weeks old were purchased from The Jackson Laboratory, and pigs 10–12 weeks old were purchased from Professional Veterinary Research (Brownstown, IN). The animals were maintained in accord with the guidelines established by the Committee on Animals at the University of Louisville Medical School.

**Models of Laser-Induced CNV.** C57BL/6 mice were anesthetized with a mixture of ketamine/xylazine (8:1), and the pupils were dilated with a single drop of 1% tropicamide. Krypton red laser photocoagulation (50- $\mu$ m spot size, 0.05-s duration, 250 mW) was used to generate three laser spots in each eye surrounding the optic nerve by using a hand-held coverslip as a contact lens. A bubble formed at a laser spot indicated rupture of the Bruch's membrane. The laser spots were evaluated for the presence of CNV on day 7 or 17 after laser treatment, using confocal microscopy.

We modified this protocol to induce CNV in pigs by using the indirect diode laser to generate 10–16 laser spots in the posterior retina with a 20D lens (810 nm, 750–1,400 mW, 0.2 s). An intense focal laser spot ruptured the Bruch's membrane, resulting in an incidence of CNV >60% after 1 week.

**i.o. Injection in the Mouse.** After anesthesia and dilation of the pupil, the anterior chamber was entered via the limbus with a 28-gauge needle to decompress the eye. Under an operating microscope, which allowed visualization of the retina, a 32-gauge

Abbreviations: AMD, age-related macular degeneration; CNV, choroidal neovascularization; PNV, pathological neovascularization; TF, tissue factor; RPE, retinal pigment epithelium; i.o., intraocular; fVII, factor VII.

<sup>†</sup>To whom correspondence should be addressed. E-mail: alan.garen@yale.edu or hank.kaplan@louisville.edu.

**Table 1. Incidence of CNV formation when the adenoviral vector was administered by i.v. injection 1 and 4 days after laser treatment**

Treatment	No. of mice	Laser spots per eye	Total spots	CNV-positive spots	CNV-negative spots
Control vector	5	3	30	29 (97%)	1 (3%)
Icon vector	6	3	36	2 (5%)	34 (95%)

Laser spots were produced in C57BL/6 mice on day 0, and i.v. injections of  $2.8 \times 10^9$  VP of the control vector or the vector encoding the Icon were administered on days 1 and 4. The mice were killed on day 7. A Chi-square test of the data showed  $P < 0.0001$ .

(blunt) needle was passed through a scleral incision, just behind the limbus, into the vitreous cavity or subretinal space. A Hamilton syringe was used to inject 1  $\mu$ l of fluid.

**Evaluation of Laser Spots for the Presence of a CNV.** At the time of death mice were anesthetized (ketamine/xylazine mixture, 8:1) and perfused through the heart with 1 ml PBS containing 50 mg/ml fluorescein-labeled dextran (FITC-Dextran, 2 million average molecular weight, Sigma). The eyes were removed and fixed for 1 h in 10% phosphate-buffered formalin. The cornea and the lens were removed and the neurosensory retina was carefully dissected from the eyecup. Five radial cuts were made from the edge of the eyecup to the equator; the sclera-choroid-retinal pigment epithelium (RPE) complex was flat-mounted, with the sclera facing down, on a glass slide in Aquamount. Flat mounts were stained with a mAb against elastin (Sigma) and a CY3-conjugated secondary antibody (Sigma) and examined with a confocal microscope (Zeiss LSM510). The CNV stained green whereas the elastin in the Bruch's membrane stained red. A laser spot with green vessels was scored CNV-positive, and a laser spot lacking green vessels was scored CNV-negative (see Fig. 4).

**Evaluation of Toxicity.** In mice treated by i.v. injection of the vector encoding the Icon (Table 1) or of the Icon protein (see Table 5), the liver, kidneys, heart, and eyes were examined for morphological and histological evidence of toxicity.

**Synthesis of the Icon cDNA and Protein.** The cDNA encoding mouse fVII (mfVII) was synthesized by PCR from a liver cDNA library and cloned into the expression vector pcDNA 3.1 in-frame at the 3' end with the cDNA encoding the Fc region of a human IgG1 Ig (hFc). A mutation from lysine-341 to alanine was introduced into the mfVII domain by site-directed mutagenesis of the cDNA to inhibit the blood coagulation activity of the Icon (16). The vector containing the mfVII/hFc Icon was transfected into Chinese hamster ovary cells, and stable transfectants were selected in RPMI supplemented with FBS and G418. A transfected clone was grown in a serum-free medium supplemented with vitamin K1, and the Icon was purified from the medium by affinity chromatography on protein A resin (16).

**Construction and Synthesis of the Adenoviral Vector.** The adenoviral vector encoding the mfVII/hFc Icon was constructed by using the shuttle vectors pAdTrack-CMV or pShuttle-CMV and the backbone vector pAdEasy-1, and the vector particles (VP) were produced in 293 cells and purified by centrifugation in a CsCl gradient (16, 17). The concentration of VP was calculated as follows: 1.0 optical density unit at 260 nm =  $1.0 \times 10^{12}$  VP. The activity of each preparation of VP was tested for the synthesis and secretion of the Icon, as follows. Cultures of 293 cells or human melanoma cells were infected with the vector in serum-free medium supplemented with vitamin K1 and cultured for 2 days. A sample of the medium was then added to protein A

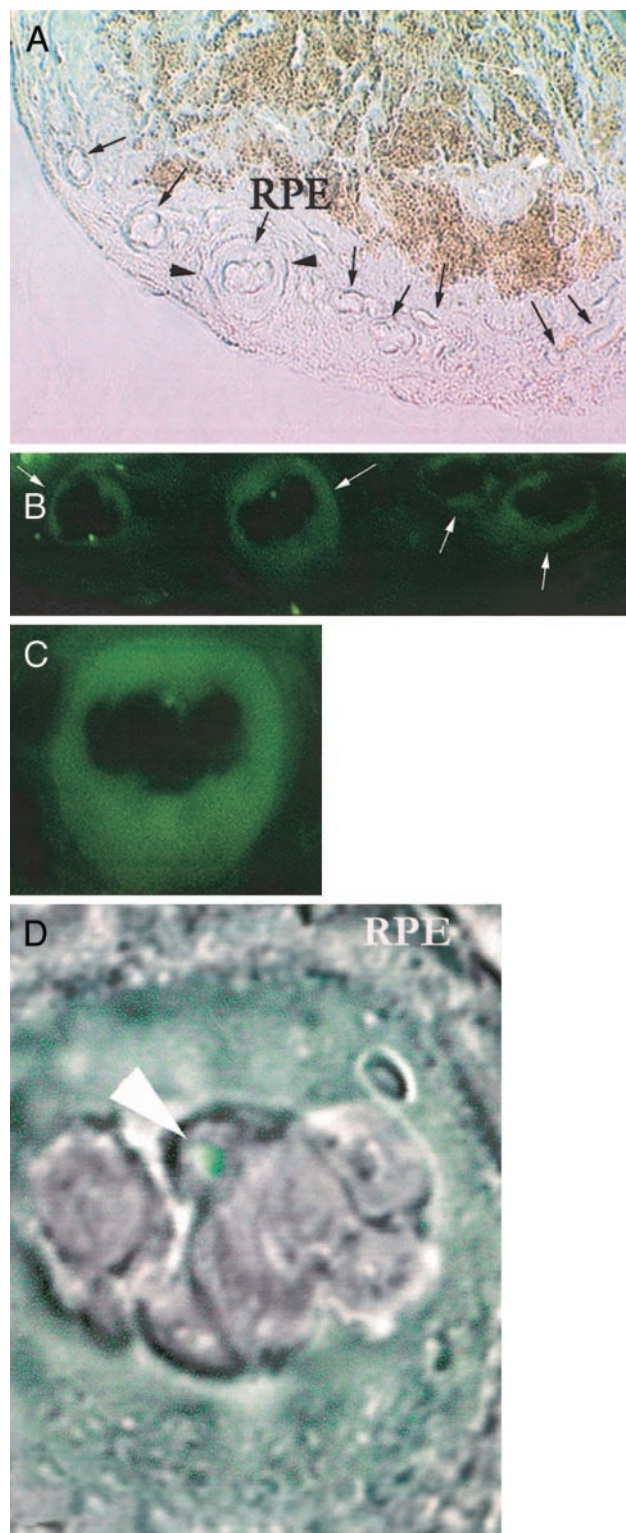


**Fig. 1.** Immunohistology of an excised human subfoveal CNV complex showing staining of the Icon. (A) Excised tissue reveals a core of RPE cells surrounded by a well-developed capillary network (black arrows). Note that capillaries surrounded by RPE cells within the core of the lesion show signs of vascular collapse and atrophy (white arrowhead) and are eventually replaced by fibrous tissue (white arrows) ( $\times 500$ ). (B) New vessels at the periphery of the CNV (white arrows) are stained intensely with the Icon ( $\times 850$ ). (C) Binding of the Icon (green stain) to the vascular endothelium of the capillary marked with black arrowheads in A ( $\times 1,500$ ). (D) Confocal micrograph of the same capillary showing speckled staining of the Icon on the endothelium ( $\times 4,500$ ). An intense signal was detected in the perinuclear endothelial cell nucleus (white arrowhead) (27).

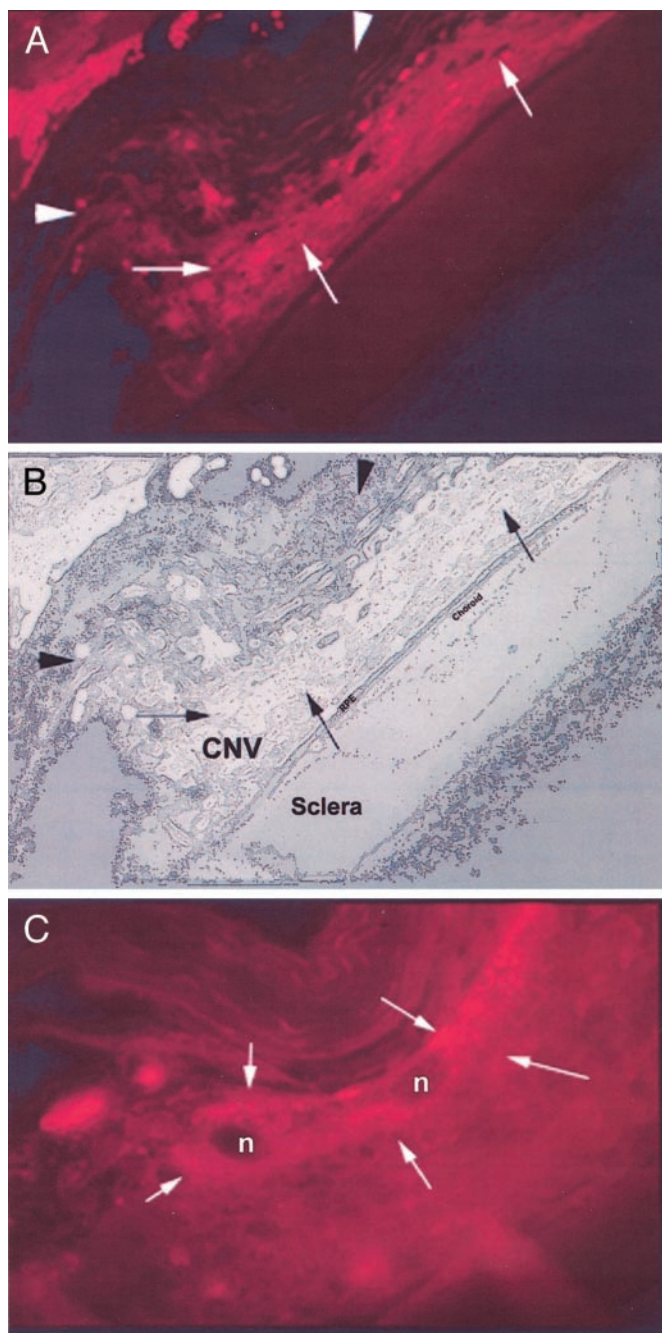


**Fig. 2.** Confocal micrograph showing immunohistologic staining of the Icon in the CNV of the mouse. (A) Laser-induced CNV stained for TF. Vascular channels are stained positively with the Icon (arrows). Autofluorescence of photoreceptors is not seen (arrow heads) due to loss of outer nuclear layer during laser photocoagulation ( $\times 100$ ). (B) Schematic diagram of laser-induced CNV complex showing RPE, choroid, and sclera. (C) Magnified view of CNV stained for TF ( $\times 600$ ). Endothelium (arrows) lining vascular channels stain for TF. Cell nuclei are indicated by n.

beads, and the bound Icon was eluted and analyzed by Western immunoblotting for Icon protein (3).

**Immunohistology.** Murine and porcine eyes were harvested immediately after the death of the animals. Human submacular CNV specimens were removed from patients with exudative AMD at the time of submacular surgery; the patients had signed an Institutional Review Board-approved permission form. Tissue samples were

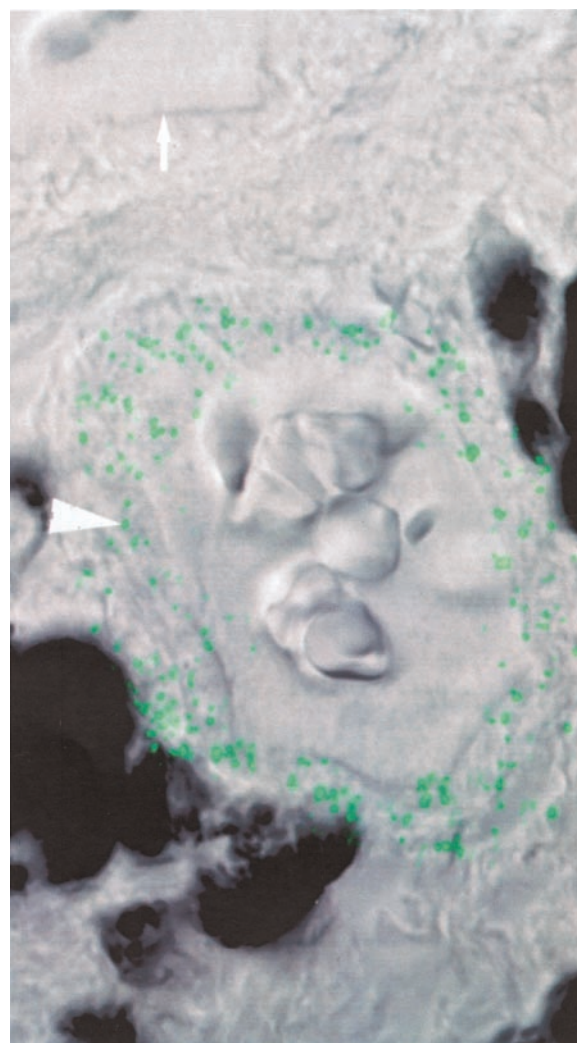


**Fig. 3.** Confocal micrograph showing immunohistologic staining of the Icon in the CNV of the pig. Choroidal flat mounts were prepared 1 week after diode laser photocoagulation in the pig, incubated with Icon protein, and stained with a FITC-labeled antibody against the Fc domain of the Icon. The endothelial cells of the CNV membrane (arrowhead) are stained green (speckled pattern), whereas the normal retinal vascular endothelium is not stained (arrow). The normal choroidal endothelium also did not stain (not shown) ( $\times 2,000$ ).

embedded in OCT compound (Tissue-Tek, Torrance, CA) and snap-frozen in liquid nitrogen. Serial frozen sections  $2 \mu\text{m}$  thick were cut through the entire tissue sample. Sections with CNV were incubated with the Icon protein for 5 h, washed with PBS, stained with FITC-conjugated antibody against the heavy chain of human IgG1, which labels the hFc domain of the Icon, and examined by light microscopy and confocal microscopy.

**Results**

**Specific Binding of the Icon to the CNV.** Sections of the choroid obtained from laser-treated mouse and pig eyes and from patients with exudative AMD at the time of submacular surgery were tested by immunohistochemistry for binding the Icon. The vessel channels of the CNV in each species showed intense staining of the Icon, in contrast to the absence of Icon staining in the normal vasculature of the choroid and retina of mice, pigs, and humans (Figs. 1–3).

**Prevention of CNV Formation.** After laser induction of multiple CNV lesions in mice, the Icon was administered by i.v. or i.o.

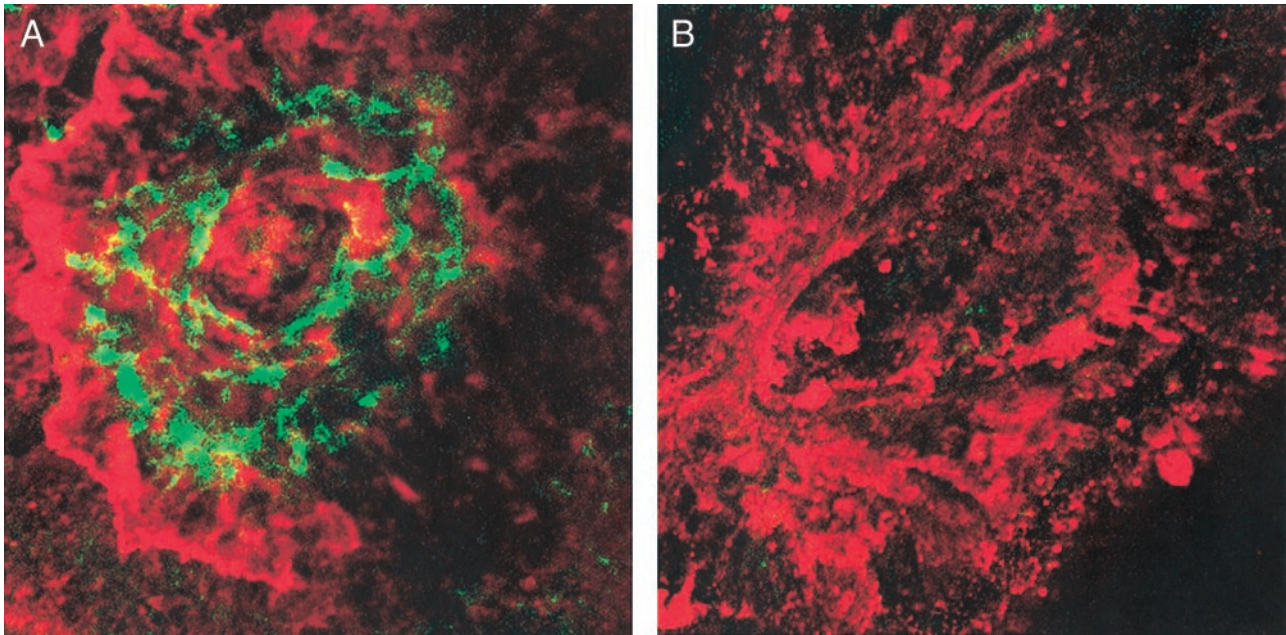


**Fig. 4.** Confocal micrograph of laser-induced CNV in the mouse. (A) Mice were injected i.v. with the control adenovirus on day 1 followed on day 7 by perfusion with FITC-Dextran. The eyes were excised and choroidal flat mounts were stained with a mAb against elastin and then with a CY3-conjugated second antibody. The prominent neovascular growth stained green whereas the underlying elastin in the Bruch's membrane stained red within a laser spot. The RPE (dark brown) was disrupted in the bed of the laser spot ( $\times 2,500$ ). (B) Mice received an i.v. injection of the adenoviral vector encoding the Icon on day 1, and choroidal flat mounts were prepared on day 7 as described above. The inhibition of new vessel growth is indicated by the absence of vessels with a green stain ( $\times 2,500$ ).

injections of an adenoviral vector encoding the Icon or of purified Icon protein. The incidence of CNV formation was determined by histochemical examination of choroidal flat mounts 7 or 17 days after laser treatment. The CNV complex stains green and the underlying elastin layer of the Bruch's membrane stains red, providing a clear identification of the CNV (Fig. 4A).

**i.v. injection of the vector.** Three laser spots were generated in each eye of 11 mice on day 0, followed by injections on days 1 and 4 of the vector encoding the Icon into six mice; a control vector that does not encode the Icon was injected into the remaining five mice. In the six mice treated with the Icon, the incidence of CNV-negative spots (Fig. 4B) was 95%, as compared with 3% in the five control mice (Table 1).

To determine the efficacy of the Icon in inducing regression of an early-stage CNV, injection of the vector was delayed until 7 days after laser induction of CNV spots. In the five mice injected with the vector encoding the Icon, the incidence of CNV-negative spots was 95%, as compared with 3% in the five control mice (Table 2).

These results indicate that i.v. injection of the adenoviral vector encoding the Icon 7 days after inducing CNV spots, which

is sufficient time for establishment of an early-stage CNV, decreased the incidence of CNV formation from 97% in the control mice to 5%.

**i.o. injection of the vector.** As an alternative to i.v. injection of an adenoviral vector encoding the Icon, which has been associated with enlarged liver cells (3), two i.o. injection routes were tested, one into the subretinal space and another into the vitreous cavity. Six mice were injected with the vector encoding the Icon and six mice were injected with the control vector, either into the subretinal space or the vitreous cavity. Among the mice treated with the Icon, the incidence of CNV-negative spots for each injection route was 72% and 83%, respectively, as compared with 22% and 12%, respectively, in the mice injected with the control vector (Table 3).

These results indicate that i.o. as well as i.v. injection of the adenoviral vector encoding the Icon is strongly efficacious in preventing CNV formation in the mouse model.

**i.v. or i.o. injection of Icon protein.** Because the efficacy of the adenoviral vector depends on secretion of the Icon protein, we tested injecting the Icon protein directly into the systemic

**Table 2. Incidence of CNV formation when the adenoviral vector was administered by i.v. injections 7 and 14 days after laser treatment**

Treatment	No. of mice	Laser spots per eye	Total spots	CNV-positive spots	CNV-negative spots
Control vector	5	3	30	29 (97%)	1 (3%)
Icon vector	5	3	30	2 (5%)	28 (95%)

Laser spots were produced in C57BL/6 mice on day 0, and i.v. injections of  $2.8 \times 10^9$  VP of the control vector or the vector encoding the Icon were administered on days 7 and 14. The mice were killed on day 17. A Chi-square test of the data showed  $P < 0.0001$ .

**Table 3. Incidence of CNV spots when the adenoviral vector was administered by i.o. injection 1 day after laser treatment**

Treatment	No. of mice	Laser spots per eye	Total spots	CNV-positive spots	CNV-negative spots
Control vector	3 (SR)	3	18	14 (78%)	4 (22%)
	3 (IVIT)	3	18	16 (88%)	2 (12%)
Icon vector	3 (SR)	3	18	5 (27%)	13 (72%)
	3 (IVIT)	3	18	3 (17%)	15 (83%)

Laser spots were produced in C57BL/6 mice on day 0, and i.o. injections of  $2.8 \times 10^8$  VP of the control vector or the vector that encodes the Icon were administered on day 1. The injections were done into the subretinal space (SR) or vitreous cavity (IVIT). The mice were killed on day 7. A Chi-square test of the data showed  $P < 0.003$  (SR) and  $P < 0.0001$  (IVIT).

**Table 4. Incidence of CNV spots when 10  $\mu\text{g}$  of Icon protein was administered by i.v. injection 1 day after laser treatment**

Treatment	No. of mice	Laser spots per eye	Total spots	CNV-positive spots	CNV-negative spots
Human IgG1	3	3	18	15 (83%)	3 (17%)
Icon protein	3	3	18	10 (56%)	8 (44%)

Laser spots were produced in C57BL/6 mice on day 0, and an i.v. injection of 10  $\mu\text{g}$  of a human IgG1 control or Icon protein was administered on day 1. The mice were killed on day 7. A Chi-square test of the data showed  $P = 0.07$ .

circulation. The incidence of CNV-negative spots was 44% in the three mice injected i.v. with 10  $\mu\text{g}$  of Icon protein, as compared with 17% in the three mice injected with an IgG1 control (Table 4). When the amount of Icon protein was increased to 50  $\mu\text{g}$ , the incidence of CNV-negative spots increased to 89% as compared with 11% for the IgG1 control (Table 5).

The Icon protein also was tested by i.o. injection into the vitreous cavity. Injecting 1.5  $\mu\text{g}$  of Icon protein resulted in 90% CNV-negative spots, as compared with an average of 7% in the controls (Table 6).

These results indicate that i.v. injection of 50  $\mu\text{g}$  of Icon protein or i.o. injection of 1.5  $\mu\text{g}$  of Icon protein is strongly efficacious in preventing CNV formation in the mouse model. **Toxicity examination.** Morphological and histological examination of the liver, kidneys, heart, and eyes of the Icon-treated mice at autopsy did not show evidence of toxicity.

## Discussion

AMD is the leading cause of blindness after age 55 in the industrialized world. The exudative form of AMD, which generates a leaky CNV causing damage to the overlying retina usually involving the macular region, is responsible for most cases of sudden and disabling loss of central vision (18,19). The main treatments currently in use or under development for exudative AMD include photodynamic therapy (10), submacular surgery (11, 12), macular translocation (13–15), and transplantation (21). However, none of these treatments restore lost central vision in most patients and can result in significant complications (19–21). Other therapeutic strategies involve administering pharmacologic agents that inhibit angiogenesis, including an antiangiogenic corticosteroid, an antibody against vascular endothelial growth factor (VEGF) (22), and a VEGF aptamer (23).

Here we described a procedure for destroying a CNV by administering an Icon molecule that binds to TF with higher affinity and specificity than can be achieved with an anti-TF antibody. TF is expressed on endothelial cells of the CNV but not of normal ocular blood vessels (see Figs. 1–3) and therefore could provide a selective and accessible target for immunotherapy of exudative AMD. Although TF also is expressed on cells of several organs and tissues, including brain, lung, and kidney

**Table 5. Incidence of CNV spots when 50  $\mu\text{g}$  of Icon protein was administered by i.v. injection 1 day after laser treatment**

Treatment	No. of mice	Laser spots per eye	Total spots	CNV-positive spots	CNV-negative spots
Human IgG1	3	3	18	16 (89%)	2 (11%)
Icon protein	3	3	18	2 (11%)	16 (89%)

Laser spots were produced in C57BL/6 mice on day 0, and an i.v. injection of 50  $\mu\text{g}$  of a human IgG1 control or Icon protein was administered on day 1. The mice were killed on day 7. A Chi-square test of the data showed  $P < 0.0001$ .

**Table 6. Incidence of CNV spots when Icon protein was administered by i.o. injection 1 day after laser treatment**

Treatment	No. of mice	Laser spots per eye	Total spots	CNV-positive spots	CNV-negative spots
PBS	8	3	48	44 (92%)	4 (8%)
Human IgG1	8	3	48	45 (94%)	3 (6%)
Icon protein	8	3	48	5 (10%)	43 (90%)

Laser spots were produced in C57BL/6 mice on day 0, and an i.o. (intravitreal) injection of 1  $\mu\text{l}$  of PBS or human IgG1 (1.5  $\mu\text{g}/\mu\text{l}$ ) as controls or with 1  $\mu\text{l}$  of Icon protein (1.5  $\mu\text{g}/\mu\text{l}$ ) was administered on day 1. The mice were killed on day 7. A Chi-square test of the data showed  $P < 0.0001$ .

glomeruli, these sites are not normally accessible to the Icon because the tight endothelial cell layer in normal blood vessels acts as a barrier. The Icon is a chimeric antibody-like molecule composed of fVII, the natural ligand for TF, conjugated to the Fc region of an IgG1 Ig. The Fc region binds and activates components of the immune system, including natural killer cells and complement (9) that are functional within the eye (24, 25), causing a cytolytic immune attack against cells that bind the Icon. Cytolysis of the CNV endothelium mediated by the Icon can result in the destruction of the associated CNV (see Fig. 4), similar to the destruction of the PNV in solid tumors (3, 4).

The efficacy and safety of the Icon for immunotherapy of laser-induced CNV was tested in a mouse model, using two procedures to administer the Icon. One procedure involves synthesis of the Icon *in vivo* by injection of an adenoviral vector encoding the Icon, and another procedure involves injection of purified Icon protein. The vector and the Icon protein were administered by i.v. injections or i.o. injections into the vitreous cavity or subretinal space of the eye. When the vector was administered by i.v. injection on the first or seventh day after laser induction of a CNV, the incidence of CNV formation was reduced from 97% to 5% (see Tables 1 and 2). Similar results were obtained by injecting the vector directly into the vitreous cavity or subretinal space of the eye (see Table 3). Administering the Icon by i.v. injection of 50  $\mu\text{g}$  of Icon protein or i.o. injection of 1.5  $\mu\text{g}$  of Icon protein also resulted in a strong reduction of CNV formation (see Tables 4–6). No toxic effects were observed by histologic examination of the liver, kidney, heart, and eye at 7 days after i.v. injection of the vector encoding the Icon or of the Icon protein. It is particularly significant that the RPE and choroid in the eye appeared normal, except for the minute spots of laser-induced damage, suggesting that the Icon can prevent CNV formation without associated damage to the eye. Thus, the Icon could be administered effectively and safely either encoded in an adenoviral vector or as a purified Icon protein, using either an i.v. or i.o. route of injection. For the experiments in mice, the Icon contained a mouse fVII domain that binds with high affinity and specificity to mouse TF expressed by a mouse CNV. For experiments with other species, and for clinical applications, the Icon would contain the autologous fVII and Fc domains, to optimize binding to TF and minimize the potential immunogenicity of the Icon.

A potential clinical application of the Icon is to prevent the development of a CNV in high-risk patients with moderate or severe nonexudative (dry) AMD (26), who are expected to retain their central vision after treatment. Another application is to resolve a CNV that has already developed in one or both eyes, causing progressive loss of central vision. In the mouse model the Icon prevented CNV formation when the first injection of the vector encoding the Icon occurred 7 days after laser induction of a CNV (see Table 2), providing sufficient time for a CNV to become established before treatment. The Icon could have a similar effect for AMD patients with an established CNV.

Support for the laboratory of H.J.K. was provided in part by the National Institutes of Health, Research to Prevent Blindness Inc. NY, and Commonwealth of Kentucky Research Challenge Trust Fund. Support

for the laboratory of A.G. was provided in part by a Program Project grant from the National Institutes of Health and by the International Retinal Research Foundation.

1. Folkman, J. (1995) *N. Engl. J. Med.* **333**, 1757–1763.
2. Kaplan, H. J., Leibole, M. A., Tezel, T. & Ferguson, T. A. (1999) *Nat. Med.* **5**, 292–297.
3. Hu, Z. & Garen, A. (2000) *Proc. Natl. Acad. Sci. USA* **97**, 9221–9225.
4. Hu, Z. & Garen, A. (2001) *Proc. Natl. Acad. Sci. USA* **98**, 12180–12185.
5. Birchler, M., Viti, F., Zardi, L., Spiess, B. & Neri, D. (1999) *Nat. Biotechnol.* **17**, 984–988.
6. Hood, J., Bednarski, M., Frausto, R., Guccione, S., Reisfeld, R. A., Xiang, R. & Cheresch, D. A. (2002) *Science* **296**, 2404–2407.
7. Drake, T. A., Morrissey, J. H. & Edgington, T. S. (1989) *Am. J. Pathol.* **134**, 1087–1097.
8. Contrino, J., Hair, G., Reutzer, D. L. & Rickles, F. (1996) *Nat. Med.* **2**, 209–215.
9. Wang, B., Chen, Y., Ayalon, O., Bender, J. & Garen, A. (1999) *Proc. Natl. Acad. Sci. USA* **96**, 1627–1632.
10. Schmidt-Erfurth, U., Miller, J. W., Sickenberg, M., Laqua, H., Barbazetto, I., Gragoudas, E. S., Zografos, L., Piguat, B., Pournaras, C. J., Donati, G., *et al.* (1999) *Arch. Ophthalmol.* **117**, 1177–1187.
11. Berger, A. S. & Kaplan, H. J. (1992) *Ophthalmology* **99**, 969–975.
12. Berger, A. S., Conway, M., Del Priore, L. V., Walker, R. S., Pollack, J. S. & Kaplan, H. J. (1997) *Arch. Ophthalmol.* **115**, 991–996.
13. Fujii, G. Y., de Juan, E., Jr., Pieramici, D. J., Humayun, M. S., Phillips, S., Reynolds, S. M., Melia, M. & Schachat, A. P. (2002) *Am. J. Ophthalmol.* **134**, 69–74.
14. Toth, C. A. & Freedman, S. F. (2001) *Retina* **21**, 293–303.
15. Aisenbrey, S., Lafaut, B. A., Szurman, P., Grisanti, S., Luke, C., Krott, R., Thumann, G., Fricke, J., Neugebauer, A., Hilgers, R. D., *et al.* (2002) *Arch. Ophthalmol.* **120**, 451–459.
16. Hu, Z., Sun, Y. & Garen, A. (1999) *Proc. Natl. Acad. Sci. USA* **96**, 8161–8166.
17. He, T. C., Zhou, S., DaCosta, L. T., Yu, J., Kinzler, K. W. & Vogelstein, B. (1998) *Proc. Natl. Acad. Sci. USA* **95**, 2509–2514.
18. Ferris, F. L., III, Fine, S. L. & Hyman, L. A. (1984) *Arch. Ophthalmol.* **102**, 1640–1642.
19. Fine, S. L., Berger, J. W., Maguire, M. G. & Ho, A. C. (2000) *N. Engl. J. Med.* **342**, 483–492.
20. Bressler, N. M. (2001) *Arch. Ophthalmol.* **119**, 198–207.
21. Algere, P. V., Berglin, L., Gouras, P., Sheng, Y. & Kopp, E. D. (1997) *Graefes Arch. Clin. Exp. Ophthalmol.* **235**, 149–158.
22. Krzystolik, M. G., Afshari, M. A., Adamis, A. P., Gaudreault, J., Gragoudas, E. S., Michaud, N. A., Li, W., Connolly, E., O'Neill, C. A. & Miller, J. W. (2002) *Arch. Ophthalmol.* **120**, 338–346.
23. The Eyetech Study Group (2002) *Retina* **22**, 143–152.
24. Sohn, J.-H., Kaplan, H. J., Suk, H.-J., Bora, P. S. & Bora, N. S. (2000) *Invest. Ophthalmol. Visual Sci.* **41**, 3492–3502.
25. Sohn, J.-H., Kaplan, H. J., Suk, H.-J., Bora, P. S. & Bora, N. S. (2000) *Invest. Ophthalmol. Visual Sci.* **41**, 4195–4202.
26. Age-Related Eye Disease Study Group (2001) *Arch. Ophthalmol.* **119**, 1417–1436.
27. Schectet, A. D., Giesen, P. L. A., Taby, O., Rosenfield, C.-L., Rossikhina, M., Fyfe, B. S., Kohtz, D. S., Fallon, J. T., Nemerson, Y. & Taubman, M. B. (1997) *J. Clin. Invest.* **100**, 2276–2285.